Environmental Science
Water Research & Technology

ROYAL SOCIETY OF CHEMISTRY

PAPER

View Article Online
View Journal | View Issue

Cite this: *Environ. Sci.: Water Res. Technol.*, 2024, **10**, 1890

Development of composite alginate bead media with encapsulated sorptive materials and microorganisms to bioaugment green stormwater infrastructure†

Debojit S. Tanmoy[ab] and Gregory H. LeFevre *[ab]

Green stormwater infrastructure (GSI) is being increasingly implemented in urban areas as a nature-based solution to improve water quality and increase groundwater recharge. Nevertheless, GSI is inefficient at removing many trace organic contaminants (TOrCs) and dissolved nutrients, potentially risking groundwater contamination. We developed and characterized novel engineered geomedia to rapidly capture stormwater pollutants *via* sorption, including TOrCs and dissolved nutrients, while bioaugmenting microorganisms to subsequently degrade captured contaminants in GSI. We created "BioSorp Bead" geomedia by encapsulating powdered activated carbon [PAC] (sorbent), iron-based water treatment residual [FeWTR] (density, sorbent), wood flour [WF] (growth substrate), white-rot-fungi [WRF] (model biodegrading organism), and AQDS (model electron shuttle) in cation-alginate matrices (Ca^{2+}, Fe^{3+}). We thoroughly mixed WRF culture with autoclaved PAC, FeWTR, AQDS, and WF in 1% alginate. This mixture was added dropwise *via* peristaltic pump into 270.3 mM $CaCl_2$/$FeCl_3$ (on a platform shaker) to instantaneously form beads that were then air-dried. Encapsulated fungi remained viable in dried beads over an extended period (3 months at room temperature), demonstrating potential for bioaugmentation applications. We quantified bead physical properties (*i.e.*, surface area, pore volume, mechanical strength, swelling, leaching), demonstrating that properties can be customized by adjusting composition parameters (*e.g.*, crosslinking with $FeCl_3$ *vs.* $CaCl_2$ increased bead mechanical strength). We also conducted preliminary sorption experiments to evaluate capture potential for imidacloprid (neonicotinoid insecticide) from synthetic stormwater runoff. The envisioned goal of the BioSorp Beads is to facilitate rapid contaminant capture during infiltration of storm events and support microorganisms that subsequently degrade sorbed chemicals, thus renewing GSI sorption capacity *in situ*.

Received 10th April 2024,
Accepted 10th June 2024

DOI: 10.1039/d4ew00289j

rsc.li/es-water

Water impact

Hydrophilic trace organic contaminants and dissolved-phase nutrients can pass through traditional stormwater management systems and create risk of groundwater contamination. Biologically active sorptive media can rapidly capture many stormwater-relevant pollutants and bio-transform these contaminants to sustain contaminant removal. We developed a novel scalable media, BioSorp Beads, that can bioaugment contaminant-degrading microorganisms in stormwater infrastructure and have high pollutant sorption potential.

1. Introduction

Urban areas generate rapid and voluminous stormwater runoff during precipitation events, which contains complex mixtures of both dissolved phase and particle-bound contaminants that degrade water quality.[1] Conventional stormwater management methods are typically ineffective for removing dissolved phase contaminants (*e.g.*, dissolved phosphorus [P], polar trace organics).[1–3] Green stormwater infrastructure (GSI) is being increasingly implemented as a nature-based solution to improve urban stormwater runoff quality, increase groundwater recharge,[4–7] and address broader societal needs.[8] Bioretention cells are one of the most widely-used GSI practices.[3,9] Conventional bioretention cells are typically filled with porous media consisting of sand,

[a] *Department of Civil and Environmental Engineering, University of Iowa, 4105 Seamans Center, Iowa City, Iowa, 52242, USA. E-mail: gregory-lefevre@uiowa.edu; Tel: 319 335 5655*
[b] *IIHR—Hydroscience and Engineering, 100 C. Maxwell Stanley Hydraulics Laboratory, University of Iowa, Iowa City, Iowa, 52242, USA*
† Electronic supplementary information (ESI) available. See DOI: https://doi.org/10.1039/d4ew00289j

compost, soil, and mulch with vegetation[10] to maintain high hydraulic conductivity/infiltration rates and prevent extended ponding. These cells successfully remove particle-associated pollutants, such as suspended solids, bacteria, some nutrients, and some heavy metals.[11] Nevertheless, dissolved phase compounds that are polar and hydrophilic, including many trace organic contaminants (TOrCs), demonstrate inferior removal in conventional media[11–13] and are more likely to pass through bioretention cells.[1] Failure to capture TOrCs in conventional bioretention media can potentially risk groundwater contamination.[14–16] Therefore, improved media for bioretention cells is necessary to remove TOrCs from stormwater in GSI while protecting underlying groundwater.

Amending conventional bioretention cell media with black carbon materials can substantially improve stormwater quality by rapidly capturing polar trace organic contaminants *via* sorption. Bioretention cells containing black carbon materials (*i.e.*, biochar, granular or powdered activated carbon [GAC or PAC]), can help remove multiple different types of trace organics from stormwater runoff[17,18] *via* multiple sorption mechanisms.[19] For instance, Ulrich *et al.*[20] modified stormwater biofilters with biochar and achieved superior TOrC removal over traditional unamended biofilters. There are similar recent reports of improved high trace organic[21] and dissolved nutrient[22] removal in black carbon modified stormwater bioretention systems. Even amendment of black carbon in bioretention cells, however, does not represent a complete solution because sorption capacity can be exhausted over extended time periods. Thus, there is a growing need to develop improved media capable of degrading contaminants *in situ* to renew sorption capacities and sustain long-term pollutant removal of GSI while minimizing maintenance.

Enhancement of biological processes in GSI modified with black carbon could provide a sustained solution for the removal of captured TOrCs. Microbial uptake/metabolism can improve contaminant removal in bioretention cells by facilitating biologically-mediated redox reactions during inter-storm periods,[23] which regenerates some of the GSI media sorption capacity.[24] Therefore, biologically active sorptive media holds the potential to decouple the short hydraulic residence time in bioretention cell necessary for rapid stormwater infiltration from the longer chemical residence time needed for biodegradation of TOrCs, ensuring sustainable treatment. In addition to biodegradation, microorganisms further enhance contaminant removal *via* biotic sorption onto the biofilms.[24] Hence, biodegradation of TOrCs could be key to improvement of stormwater runoff quality though *in situ* renewal of sorption capacities of the treatment media.[25]

Studies related to contaminant biotransformation in GSI to date mainly focus around bacterial and plant processes,[26–28] while fungi are under-investigated in stormwater bioretention. White rot fungi (WRF) are a class of well-known wood decaying fungi that can produce a variety of both extracellular enzymes [*e.g.*, manganese peroxidase (MnPs), lignin peroxidase (LiPs), laccases] and intracellular enzymes [*e.g.*, CYP450][29] capable of degrading recalcitrant organic compounds.[30] Our lab recently reported[31] that WRF are capable of biodegrading some tire wear compounds, which are becoming increasingly recognized for their presence and persistence in urban stormwater and impacts to aquatic life.[32–35] WRF are also known to degrade urban-use recalcitrant pesticides (*e.g.*, *Trametes versicolor* can degrade the phenylpyrazole-based pesticide fipronil[36]). When WRF are proximal to black carbon materials, biotransformation dynamics may potentially change because the redox-active groups present on black carbon surfaces can function as redox mediators of fungal extracellular enzymes.[37] Black carbon materials can also immobilize fungal enzymes *via* adsorption onto the porous structures and by covalent bonds with the surface functional groups, resulting in higher fungal biodegradation potential.[38,39] Nevertheless, the limited research to date in bioretention has focused on fungal nutrient cycling or interactions with plants, with a distinct paucity of work on the potential to directly incorporate WRF into GSI systems.[40–42] Bioaugmenting GSI with WRF holds promise for trace organic biodegradation and improved stormwater quality, therefore representing a critical research need.

The objective of this research was to develop a novel biologically active sorptive geomedia with encapsulated white-rot fungi to bioaugment green stormwater infrastructure. Here, we encapsulated powdered activated carbon (PAC), wood flour, iron water treatment residuals (FeWTR), anthraquinone-2,6-disulfonate (AQDS), and *Trametes versicolor* as a model WRF in Ca^{2+}/Fe^{3+} alginate hydrogel structures to create "BioSorp beads". We verified fungal viability in the dried beads over an extended time period and characterized a suite of BioSorp bead physical properties (*i.e.*, surface area, pore volume, mechanical strength, swelling, leaching *etc.*). Black carbon (PAC) has multiple active adsorption sites and is well-established to sorb various trace organics and ionic contaminants.[19] Iron oxides present in iron-based water treatment residuals (FeWTR),[43] can potentially sorb dissolved phosphorus and PFAS.[44–46] Practically, FeWTR also increases the bead density to avoid floating media during precipitation events and maintains bioretention structural integrity. WRF secrete a variety of intra- and extracellular enzymes and degrade different trace organic compounds.[29,31] Wood flour acts as a carbon/energy source for fungi to maintain fungal viability for extended time periods.[47] AQDS (a commonly used model electron shuttle) can enhance the degradation of various recalcitrant organic contaminants by acting as redox mediators for microbial metabolism/contaminant transformation.[48] To the best of our knowledge, this is the first study to integrate the potentials of deploying composite fungi alginate beads in bioretention cells for the goals of field bioaugmentation and subsequent trace organic removal from urban stormwater runoff, thus representing a novel assemblage of materials and organisms. The BioSorp beads are, however, fundamentally a platform technology that could be adapted to encapsulate other microbes or materials for a suite of environmental remediation (*e.g.*, contaminated sediment

bioaugmentation) or biotechnology applications (*e.g.*, fluidized bed bioreactor).

2. Materials and methods

2.1 Chemicals, materials, and cultures

Calcium chloride, ferric chloride, sodium alginate, sodium nitrate, magnesium chloride hexahydrate and powdered activated carbon (PAC) were purchased from Fisher Scientific. Anthraquinone-2,6-disulfonate (AQDS), sodium sulfate, and sodium bicarbonate were purchased from Sigma Aldrich. Synthetic seawater was prepared by mixing 36 g "instant ocean sea salt" (TopDawg Pet Supply, USA) per liter of deionized water. The synthetic stormwater recipe can be found in the ESI† [section S1]. Ferric sludge containing iron water treatment residuals (FeWTR) was recovered from the University of Iowa water treatment plant. The ferric sludge was settled at room temperature for 24 hours. The top clear water layer was carefully removed *via* peristaltic pump to retain the bottom thickened FeWTR slurry. The remaining FeWTR slurry was first oven dried at 70 deg C for 2 days, and then powdered using mortar and pestle. The wood flour (sanding dust residual; also known as wood dust) was purchased from Shannon's Sawmill (Syracuse, New York, USA). Malt extract broth, ammonium chloride, and sodium phosphate dibasic were purchased from Research Products International. Dr. Jordyn Wolfand from the University of Portland graciously provided the white rot fungi (*Trametes versicolor*) culture.

2.2 BioSorp bead preparation overview summary

Here, we present summary development of the novel sorptive bioactive 'BioSorp beads' to amend bioretention cell media for microorganism delivery and trace organic removal from stormwater runoff *via* coupled sorption and biodegradation [Fig. 1]. The materials are combined, and organisms encapsulated using alginate as a biopolymer. Alginate is a commonly used sorbent in wastewater treatment for heavy metal and ionic dye removal[49,50] and could also be used for biofilm encapsulation and applied for bioaugmentation of GSI. Alginic acid is a natural organic polymer (anionic polysaccharide), which is found in brown algae.[51] This polymer contains abundant free hydroxyl and carboxyl groups in the polymeric chain that form irreversible crosslinking bonds with polyvalent cations[51] (*e.g.*, Ca^{2+}, Fe^{3+}, Al^{3+}). Calcium alginate beads form a two-dimensional 'egg-box' shaped structure, whereas Fe^{3+} alginate beads have a three-dimensional structure and are more porous than Ca^{2+} alginate beads.[52]

Different variations of BioSorp beads were prepared using powdered activated carbon (PAC), wood flour (WF), iron water treatment residuals (FeWTR), AQDS, and *T. versicolor* culture to probe the effects of varying material properties [Table S1†]. These materials were thoroughly mixed in varied concentrations of sodium alginate solution (0.5% to 1.5% w/v in DI water) and then added dropwise into calcium chloride (270.3 mM or 450.5 mM tested; described in detail below) or ferric chloride (270.3 mM) solution (made in DI water) using a peristaltic pump. In every 100 mL of sodium alginate solution, 1 g of PAC, 1 g of WF, and/or 1 g of FeWTR were added. PAC, wood flour, water treatment residuals, and/or fungi cells are trapped in the cross-links to form the final BioSorp beads. During the preparation process, the beakers containing calcium chloride or ferric chloride solutions were maintained on a platform shaker and constantly shaken at 50 rpm. Wet beads were then air dried on wax paper at room temperature for two to three days before being stored at room temperature. Dried beads (2.5 to 3 mm diameter) decrease in size by approximately 50% in diameter compared to wet beads (5 to 5.5 mm diameter).

To encapsulate fungi within the BioSorp beads, bead materials (*i.e.*, PAC, wood flour, and FeWTR) were autoclaved at 121 °C for 60 minutes prior to starting the bead preparation steps. DI water and 70% ethanol were flushed through the peristaltic pump tubing to clean any residue. One week before preparing the beads, the fungal strain was freshly inoculated by

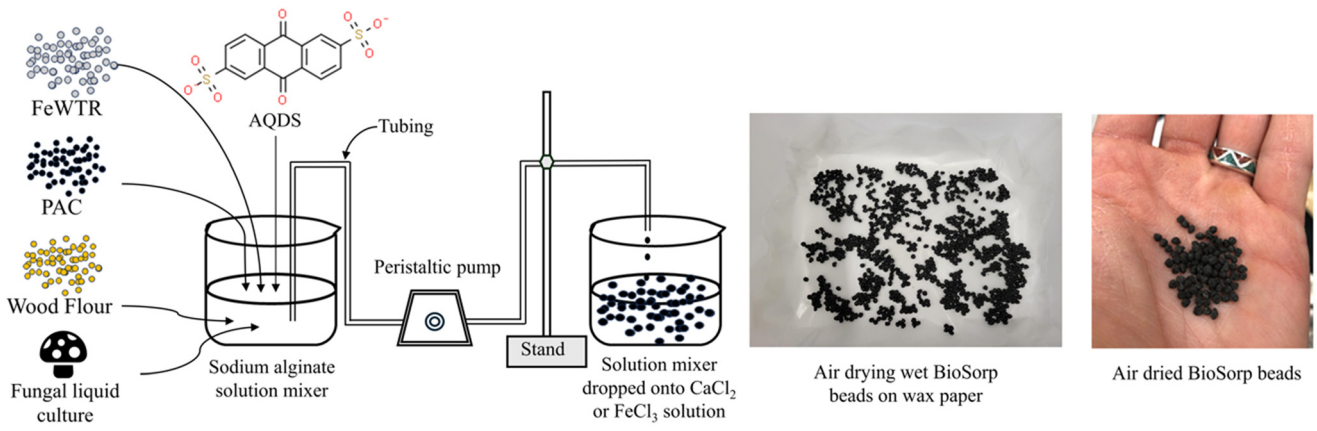

Fig. 1 Schematic diagram of BioSorp bead making procedure. The final beads containing the encapsulated materials and culture are approximately 3 mm in diameter and hard to the touch (FeWTR = iron water treatment residual; PAC = powdered activated carbon, AQDS = anthraquinone-2,6-disulfonate).

transferring into an Erlenmeyer flask containing malt extract media from an agar plate using a sterile loop. The Erlenmeyer flask was maintained on a shaker table for one week to allow sufficient fungal growth (OD_{600} ~ 1.5). After one week, the fungi culture was homogenized using a handheld OMNI homogenizer. In every 50 mL of 2% w/v sodium alginate solution, we added 50 mL homogenized fungi culture (containing fungi in malt extract media), 1 g PAC, 1 g WF, 1 g FeWTR, and 0.1 g AQDS. This mixture was thoroughly homogenized using the OMNI homogenizer to yield a 1% w/v final sodium alginate concentration in the mixture). Lastly, we added this mixture dropwise into 270.3 mM cationic (calcium chloride or ferric chloride) solution using the peristaltic pump to form the fungi containing beads. The beads were then air dried on wax paper at room temperature for two to three days.

2.3 Bead characterization experimental design

We created a suite of abiotic beads (*i.e.*, did not contain any fungal culture) to isolate and systematically vary and characterize the impacts of different preparation techniques on important physical properties of the beads (*i.e.*, varied sodium alginate concentration [0.5% to 1.5%], varied crosslinker concentration [3% *vs.* 5% $CaCl_2$], divalent/trivalent crosslinker type [$CaCl_2$ *vs.* $FeCl_3$], with *vs.* without AQDS). The systematic bead experimental design and the impacts on different measured physical properties are described in Tables 1 and S1.† We quantified the bead surface area, pore volume, and mechanical strength. We also imaged the bead surface using scanning electron microscopy (SEM). To examine the bead stability in solutions with different ionic strengths, we determined the bead swelling ratio [eqn (1)] and bead crosslinker leaching (*i.e.*, dissolved calcium and iron concentration) in deionized water, synthetic stormwater, and synthetic seawater. We maintained 100 mg of dried Fe^{3+} crosslinked alginate beads and calcium crosslinked alginate beads in 50 mL of the aforementioned solutions at room temperature, and periodically weighed the wet beads to quantify bead swelling [eqn (1)]. We also periodically measured the dissolved phase calcium or iron concentrations in the solutions.

$$\text{Bead swelling} = \frac{\text{wet bead weight} - \text{dried bead weight}}{\text{dried bead weight}} \times 100\% \quad (1)$$

We prepared two types of biologically active BioSorp beads (containing fungi; air dried beads and oven dried beads [dried at 70 deg C for 8 hours]) and stored the finished beads

Table 1 Surface area and total pore volume of different calcium-alginate and ferric-alginate beads. The linking brackets in the experimental design column highlight the testing of one variable while holding other factors constant

Experimental design			Results		
No.	Test conditions	Recipe	Surface area ($m^2\ g^{-1}$)	Total pore volume ($cm^3\ g^{-1}$)	Effect outcome summary
1		Raw PAC	787.51	0.737	
2	Varied alginate concentration	**0.5% SA** – 1% PAC – 1%WF – 270.3 mM $CaCl_2$	122.93	0.121	Alginate concentration ↑; surface area ↓; pore volume ↓;
3		**1% SA** – 1% PAC – 1%WF – **270.3 mM $CaCl_2$**	65.86	0.076	
4		**1.5% SA** – 1% PAC – 1%WF – 270.3 mM $CaCl_2$	18.17	0.019	
5	Varied crosslinker concentration	1% SA – 1% PAC – 1%WF – **450.5 mM $CaCl_2$**	27.73	0.027	Crosslinker concentration ↑; surface area ↓; pore volume ↓;
6	Varied crosslinker type	1% SA – 1% PAC – 1%WF – 1% FeWTR – **270.3 mM $FeCl_3$**	146.62	0.155	$FeCl_3$ = ↑ surface area and pore volume ; $CaCl_2$ = ↓ surface area and pore volume
7		1% SA – 1% PAC – 1%WF – 1% FeWTR – **270.3 mM $CaCl_2$**	45.24	0.052	
8	Effects of external electron shuttle	1% SA – 1% PAC – 1%WF – 1% FeWTR – **0.1% AQDS**- 270.3 mM $CaCl_2$	39.35	0.051	AQDS **marginally decreases** surface area and pore volume

at room temperature in sterile sealed tubes. The oven dried beads were prepared to determine if drying temperature impacted fungal viability. To verify the viability of the encapsulated fungi, 250 mL growth media and 2 g of freshly prepared dried BioSorp beads were combined and maintained on a platform shaker at 100 rpm for two weeks, whereupon the wet beads (and residual drops of the growth media) were imaged with an optical stereoscope to observe the fungal growth. The viability experiment was also repeated with beads stored at room temperature for three months.

2.4 Analytical methods, QA/QC, and statistical analysis

We measured bead surface area and porosity using a Quantachrome Nova 4200e BET instrument and bead mechanical strength using a molecular force probe 3D classic (MFP-3D) atomic force microscope. Dissolved calcium and dissolved iron concentrations were measured using an Agilent 7900 ICP-MS. We imaged the bead surface using Hitachi S-4800 scanning electron microscope and Olympus SZX12 Stereoscope. A more detailed description of the analytical methods can be found in section S2.† All fungal culture work was conducted in a laminar flow biosafety cabinet (BSC). The BSC was decontaminated before and after each usage with 10% (v/v) bleach, 70% (v/v) ethanol, and UV-sterilization. Fungal culture preparation and maintenance procedures were followed from our earlier work.[31] Any solution or culture not immediately needed was stored in a refrigerator at 4 °C for later usage. GraphPad Prism 9.0.0 (San Diego, CA) was used to perform all statistical analyses. Normality of the data distribution was evaluated using the Shapiro–Wilk test and normal QQ plot. When the data were significantly different from a normal or log-normal distribution (α = 0.05), non-parametric analysis was performed (*e.g.*, Mann–Whitney rank sum test rather than *t*-tests). ANOVA (α = 0.05) with Tukey *post hoc* tests were performed to quantify statistical significances among matched-paired datasets.

3. Results and discussion

3.1 Summary description of the produced geomedia

Our main objective of this phase of research was the development of sorptive engineered geomedia (BioSorp beads) that can be used as vehicles for GSI bioaugmentation. We tailored our design to employ non-toxic materials, incorporate recycled/valorized waste products, and maintain an inexpensive production process that is scalable for practical applications to field stormwater management systems. The produced beads have an extended viable shelf-life for the encapsulated organisms (at least 3 months when stored at room temperature). Previous literature indicates that white rot fungi can remain highly viable in calcium alginate beads for at least one year when stored at 5° Celsius.[47] The BioSorp bead design is intended to rapidly capture a spectrum of environmentally relevant dissolved stormwater pollutants and to bioaugment contaminant degrading microorganisms in GSI, thereby facilitating trace organic contaminant biodegradation while renewing the GSI's sorption capacities. Furthermore, the BioSorp beads are mechanically robust and appear sufficiently stable to even sustain high ionic strength stormwater runoff (*i.e.*, relevant in winter when high amounts of de-icing salts are applied), as we detail below.

The final produced dried BioSorp beads, designed for bioaugmentation and contaminant capture/bioremediation, are approximately 2.5–3 mm in diameter [Fig. 1]. This physical size is desirable to maintain high hydraulic conductivity in GSI systems. The Ca^{2+} alginate beads are spherical when freshly prepared, whereas the Fe^{3+} alginate beads generate a more disk-like/spheroidal shape, indicating denser crosslinks due to the presence of trivalent iron ions. The 'final' beads all contain PAC (to rapidly capture different trace organics), white rot fungi (as a model organism to bioaugment the bioretention cells, enabling contaminant biodegradation), wood flour (to support and maintain fungal growth), AQDS (as a redox mediator), and FeWTR (to increase bead density as well as dissolved nutrient and PFAS removal). We produced and tested multiple bead iterations with different combinations before optimizing the final bead recipe. The recipe of all the bead iterations can be found in Table S1.† Regardless of composition, alginate beads crosslinked with calcium chloride had higher pH (around 6 to 6.5) than beads crosslinked with ferric chloride (around 3.3 to 3.6). The details of different bead properties and the bead geomedia potential to bioaugment green stormwater infrastructure are described below.

3.2 Physical properties of BioSorp beads

3.2.1 Effects of bead composition on surface area and pore volume. We systematically probed the effects of alginate and cationic crosslinker concentration on bead surface area and porosity [Table 1 and Fig. 2]. We observed a substantial decrease in surface area from the original PAC to the beads (approximately 5- to 43-fold decrease). This loss of surface area for the beads compared to the PAC is attributed to the encapsulation of PAC in the alginate gel structure, and is entirely expected based on the literature.[53] Similar surface area decreases are also reported in other activated carbon hydrogel beads[53] (*e.g.*, unencapsulated activated carbon surface area was 897.9 $m^2\ g^{-1}$, whereas a chitosan bead containing the activated carbon had a surface area of 165.8 $m^2\ g^{-1}$). Both the surface area and pore volume of the BioSorp beads decreased with increasing alginate concentrations in the recipe, likely due to the denser crosslinked structures.[54] When we increased the sodium alginate (SA) concentration of the beads from 0.5% to 1%, the surface area decreased by 46%. Surface area further decreased when the alginate concentration was raised to 1.5%. We also observed similar effects when we increased the crosslinker concentrations. Beads made with 5% $CaCl_2$ (450.5 mM) had 57.9% lower surface area than the beads made with 3% $CaCl_2$ (270.3 mM). Beads created with equimolar ferric

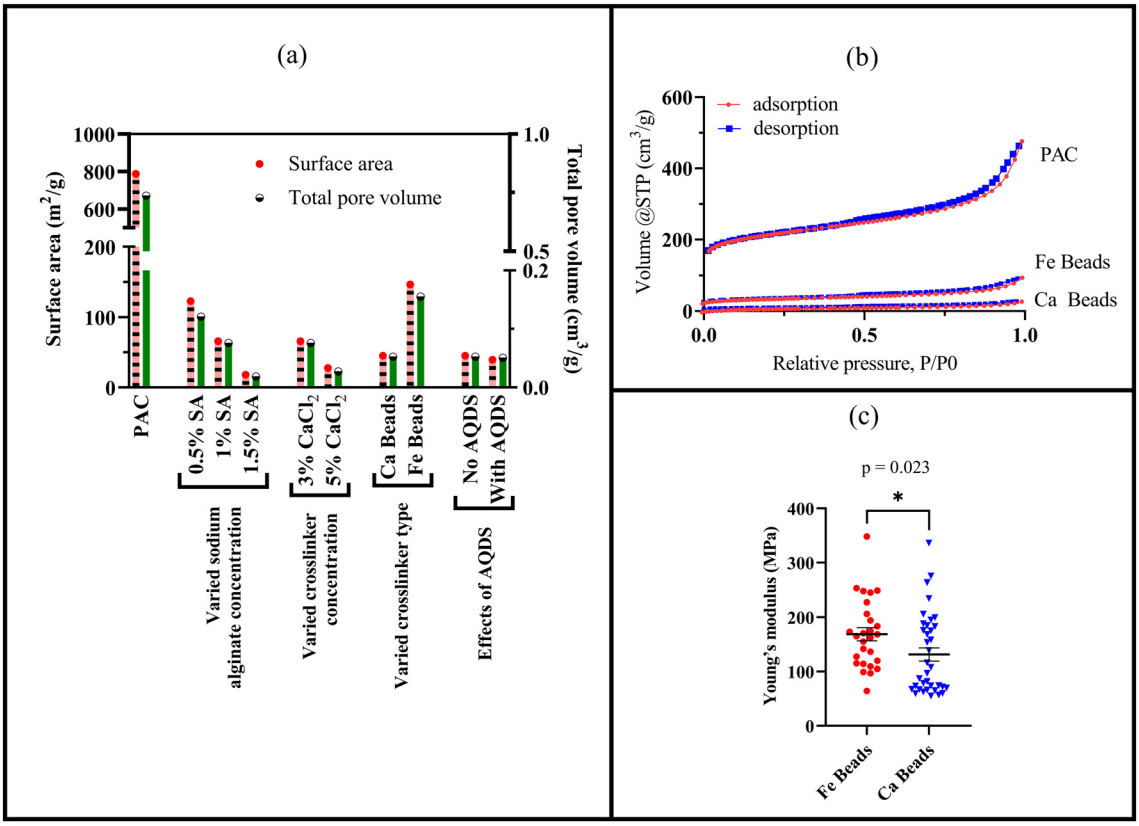

Fig. 2 (a) Effects of systematically varying bead compositions on the surface area and the total pore volume of different BioSorp beads. Compositions: (1) varied sodium alginate (SA) concentration [crosslinker concentration was constant (3% $CaCl_2$)], (2) varied crosslinker concentration [sodium alginate concentration was constant (1%); 3% $CaCl_2$ = 270.3 mM $CaCl_2$; 5% $CaCl_2$ = 450.5 mM $CaCl_2$], (3) varied crosslinker type [equimolar concentrations of $CaCl_2$ and $FeCl_3$ (270.3 mM); sodium alginate concentration was constant (1%)], and (4) beads including/excluding AQDS [both sodium alginate (1%) and crosslinker concentrations (3% $CaCl_2$) were constant]. (b) BET adsorption–desorption isotherms for PAC, Fe beads, and Ca beads. (c) Mechanical strengths (Young's modulus measurements) of Fe^{3+} alginate beads and Ca^{2+} alginate beads (n = 5; multiple measurements made on 5 beads of each type; p-value calculated from non-parametric Mann–Whitney rank sum test).

chloride (270.3 mM $FeCl_3$) crosslinker had a higher surface area (69.1% higher) and total pore volume (66.2% higher) than beads made with calcium chloride (270.3 mM $CaCl_2$). Ferric-alginate beads have three-dimensional binding structures and calcium-alginate beads have two-dimensional planar binding structures.[52] Therefore, we hypothesize that the two-dimensional planar structures in calcium-alginate beads result in lower porosity than ferric-alginate beads.

Hence, surface area and pore volumes can be customized by either adjusting the alginate concentration or the crosslinking concentration or the crosslinker type [Fig. 2(a)]. We systematically demonstrated the effects of increasing alginate and/or increasing crosslinker concentrations using the calcium alginate beads for testing for testing a single variable. Changes in surface area and pore volume would be also entirely expected for ferric cross-linked alginate beads if the alginate and/or $FeCl_3$ concentrations were changed.[54] Because of the three-dimensional binding structures in ferric cross-linked alginate hydrogel *versus* the two-dimensional binding structures in calcium cross-linked alginate,[52] the surface area and pore volume values will likely be different for these two types of composite alginate beads. Nevertheless, the key point that BioSorp bead surface area and pore volume can be customized according to the needs by changing the bead recipe remains consistent. We conclude that the ferric cross-linked alginate beads are likely to be better candidates for most GSI applications due to the higher porosity and surface area. When we added AQDS to the bead recipe (using calcium alginate as test beads), surface area and pore volume of the AQDS containing beads decreased marginally by 13% and 3.3%, respectively, compared to the beads that did not contain any AQDS. AQDS is a model quinone substance that can facilitate microbial and abiotic degradation of various recalcitrant trace organics by facilitating e^- transfer.[55–58] Considering potential for the added benefits external electron shuttles provide, we hypothesize that the presence of AQDS would likely have a net positive impact on the bead performance and AQDS should be included in the recipe. Future research will evaluate biodegradation in the presence the exogenous electron shuttle addition.

As a quality assurance measure, we characterized the BET adsorption isotherms (volume of nitrogen gas adsorbed by PAC, ferric-alginate beads, and calcium-alginate beads as a function of relative pressure), which were used to quantify

bead surface areas and pore volumes [Fig. 2(b)]. All isotherms followed IUPAC type IV (a) isotherms, where capillary condensation and hysteresis coexist. We observed capillary condensation (gas phase transitions into liquid phase) and hysteresis (adsorption and desorption pathway do not overlap) in our alginate gel bead isotherms. The hysteresis loop follows loop type H4, where noticeable adsorption at low relative pressure indicates micropore filling. This type of isotherm occurs when mesopores larger than 4 nm are present in the structures. Type IV (a) isotherms and H4 loops are common in activated carbons[59] and oxide gels like zeolite.[60]

3.2.2 Effects of bead composition on mechanical strength. Fe^{3+} alginate beads possess higher mechanical strength than Ca^{2+} alginate beads [Fig. 2(c)]. Mean values for the Young's modulus of our Fe^{3+} beads and Ca^{2+} beads were 169.7 MPa and 131.4 MPa, respectively (p = 0.023). Because the trivalent Fe^{3+} binds to both polyguluronate (GG) and polymannuronate (GM) groups of alginates in a porous three-dimensional structure, ferric alginate beads form stronger bonds than calcium alginate beads (calcium binds to the GG groups only).[52] As a result, Fe^{3+} beads have higher mechanical strength and higher porosity [Fig. 2] and swell less than Ca^{2+} beads [Fig. 4]. The Young's moduli of our BioSorp beads (made with 1% alginate; encapsulated 1% PAC, 1% WF, and 1% FeWTR) are 36 to 850 times higher than the typical reported[61,62] mechanical strengths of alginate beads containing no amendments (*i.e.*, nothing encapsulated; beads made with 10% alginate concentration exhibited a Young's modulus of 3.6 Mpa,[62] whereas the values for 2% to 5% alginate beads ranged from 0.2 MPa to 0.6 MPa).[61] Other organic hydrogel beads are reported to have even lower mechanical strength than alginate beads (*e.g.*, 1.5% chitosan bead have a reported Young's modulus of 0.187 MPa).[63] This finding indicates that the bioretention cells would likely be able to maintain structural integrity (*i.e.*, not to subside) if BioSorp beads were incorporated in the cell media.

3.2.3 SEM Microscopy to characterize bead surface. We also analyzed the surface morphology of the dried composite alginate beads using scanning electron microscopy for visual characterization (images are presented at equal magnification; scale bar = 50 μm) [Fig. 3]. All types of beads have rough and porous surface structures containing multiple cracks and pores (many >10 μm). When the sodium alginate concentration was increased in the calcium alginate bead recipe (0.5 to 1.5% sodium alginate), thicker and smoother alginate gel structures formed.[64] We observed similar effects when we increased the crosslinker concentration (3% to 5% $CaCl_2$). When we changed the crosslinker cation composition from $CaCl_2$ to $FeCl_3$, we noted a denser alginate coating with many large cracks and pores. Similarly rough and porous surfaces of composite alginate beads are also reported in previous studies.[65] Additional SEM images can be found in the ESI† section [Fig. S13].

3.2.4 Bead swelling. Calcium alginate beads swelled more than ferric alginate beads when in the presence of a high ionic strength solution [Fig. 4]. We observed that calcium alginate beads did not swell differently in DI water and in synthetic stormwater (p > 0.9999); however, the Ca^{2+} beads

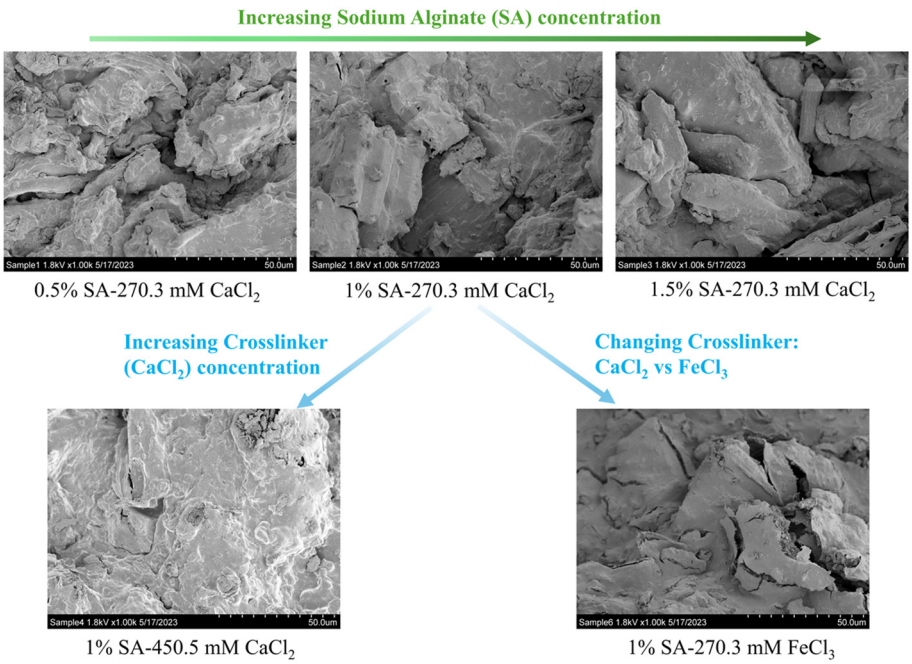

Fig. 3 Effects of varying bead compositions on the bead surface (SEM image scale bar = 50 μm). Increasing sodium alginate concentration smoothed the bead surface (crosslinker concentration was constant). Increasing the crosslinker concentration (3% to 5% $CaCl_2$) or changing the crosslinker to $FeCl_3$ from $CaCl_2$ also smoothed the bead surface (sodium alginate concentration was constant). Large cracks and pores were evident in beads crosslinked with $FeCl_3$.

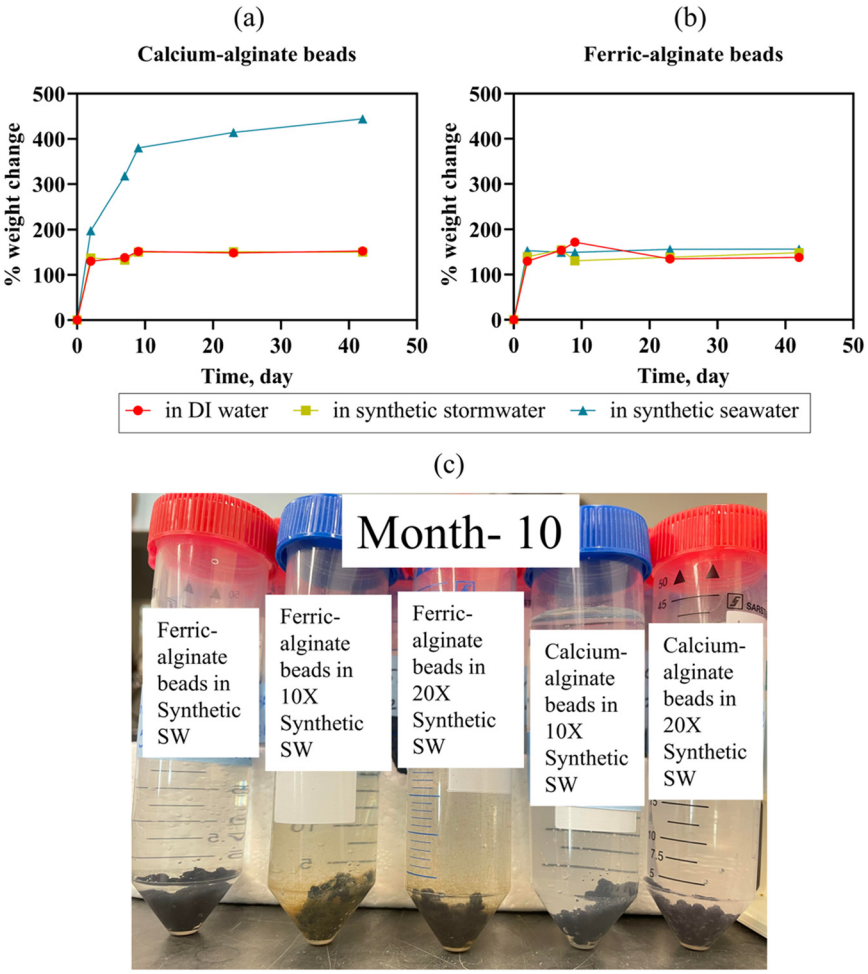

Fig. 4 (a) and (b) Percent change in weight of calcium-alginate and ferric-alginate beads, kept in DI water, synthetic stormwater, and synthetic seawater (Bead swelling: eqn (1)). Error bars represent the standard deviation of the mean (n = 2 experimental replicates; error bars too small to be visible are obscured by the data points). (c) Ferric-alginate beads and calcium-alginate beads do not disintegrate in synthetic stormwater (ionic strength = 0.005 M), 10× synthetic stormwater (ionic strength = 0.046 M), 20× synthetic stormwater (ionic strength = 0.093 M) even after 10 months.

swelled ~3 times more in synthetic seawater than in synthetic stormwater (p = 0.0372). Conversely, Fe^{3+} alginate beads exhibited similar swelling under the three ionic strength conditions tested (p = 0.9684). There were no significant differences when comparing swelling of Ca^{2+} alginate beads and Fe^{3+} alginate beads in DI water (p = 0.9742) and in synthetic stormwater (p = 0.9651); however, when the solution ionic strength increased to the level of synthetic seawater, the Ca^{2+} alginate beads swelled approximately 3 times more than Fe^{3+} alginate beads (p = 0.0476). Synthetic seawater had 140 times greater ionic strength than synthetic stormwater (0.7 M *vs.* 0.005 M). The trivalent Fe^{3+} beads have a complex three-dimensional Fe^{3+}-alginate structure, whereas the divalent Ca^{2+} beads have two-dimensional Ca^{2+}-alginate structure.[52] The Fe^{3+}-alginate structure contains a higher density of crosslinking bonds than Ca^{2+}-alginate structure, resulting in stronger beads with a lower swelling property.[52] Analogous trends in swelling results have also been reported for trivalent Al^{3+} alginate beads compared with divalent Ca^{2+} alginate beads.[66] Because both Ca^{2+} beads and Fe^{3+} beads swelled approximately the same amount in synthetic stormwater (p = 0.9651; the relative difference in swelling ratios were <2% after 42 days), both types of beads will also likely exhibit similar swelling in most relevant GSI applications. For potential applications where the beads would be exposed to high ionic strength conditions such as bioremediation/bioaugmentation of sediments in estuaries, Fe^{3+} beads may be a better choice than Ca^{2+} beads.

3.2.5 Bead leaching. Calcium alginate beads were maintained in DI water, synthetic stormwater, and synthetic seawater to quantify calcium release in the dissolved phase. There was a net increase in dissolved calcium concentration in the DI water of ~57 mg L^{-1} after 22 days (initial Ca concentration = 0.73 mg L^{-1}; Ca concentration after 22 days = 57.5 mg L^{-1}). The dissolved Ca concentration in synthetic stormwater also increased by ~22 mg L^{-1} after 22 days (initial concentration = 47.1 mg L^{-1}; Concentration after 22 days =

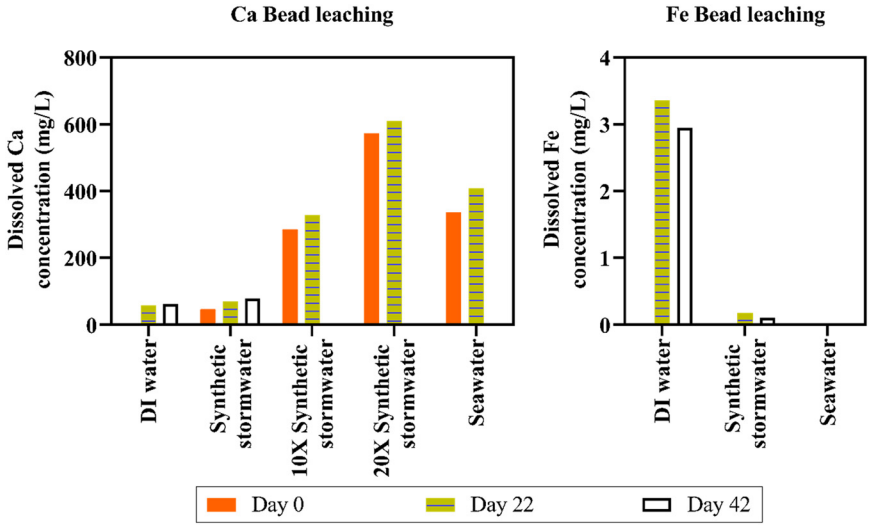

Fig. 5 Dissolved calcium concentration [leaching from Ca beads] and dissolved iron concentration [leaching from Fe beads] in solutions with different ionic strength (n = 1). 10× synthetic stormwater, 20× synthetic stormwater, and synthetic seawater data could not be collected on day 42.

69.6 mg L^{-1}), and in synthetic seawater the dissolved Ca concentration increased by ~71 mg L^{-1} (initial concentration = 337.21 mg L^{-1}; Concentration after 22 days = 408.4 mg L^{-1}) [Fig. 5 and Table S2†].

Separate mechanisms likely contributed to leaching in the different types of solutions. We hypothesize that the ~57 mg L^{-1} increase in DI water Ca concentration was due to osmotic pressure equilibrium (*i.e.*, ion concentration gradient induced from the deionized water). Conversely, ion exchange likely facilitated Ca leaching in synthetic stormwater and seawater, a process known to impact crosslinker leaching.[66] Indeed, calcium leaching was lower in synthetic stormwater (~22 mg L^{-1} dissolved Ca concentration increase in 22 days) than in high ionic strength seawater (~71 mg L^{-1} dissolved Ca concentration increase in 22 days). To ensure the beads remained stable in different ionic strength runoff, we maintained beads in DI water, synthetic stormwater, 10× synthetic stormwater, 20× synthetic stormwater, and synthetic seawater for 10 months; the beads did not disintegrate [Fig. 4(c) and S10†]. We tested leaching for all the ionic strength conditions for Ca beads as part of the experimental design. Because we did not observe any leached dissolved iron in seawater, which has a significantly higher ionic strength (0.7 M) than 10× synthetic stormwater (0.046 M) and 20× synthetic stormwater (0.093 M), we tested Fe bead iron leaching only in DI water, synthetic stormwater, and synthetic seawater [Fig. 5]—representing both the most extreme and environmentally relevant conditions. BioSorp beads are likely stable under environmentally relevant conditions for stormwater systems, such as typical freshwater up to road salt induced deicing influxes.

Iron release from Fe^{3+} alginate beads was lower than calcium release from Ca^{2+} alginate beads (*e.g.*, after 42 days, dissolved iron concentration in synthetic stormwater was ~20 times lower than dissolved calcium concentration in synthetic stormwater) [Fig. 5]. We hypothesize that the stronger bonds between trivalent iron and alginate improve bead durability (*i.e.*, less swelling/leaching). Dissolved total iron concentrations in DI water were 0.003 mg L^{-1} on day 0, 3.36 mg L^{-1} on day 22 (increased 1120-fold), and 2.95 mg L^{-1} on day 42 (increased 983-fold). In synthetic stormwater, iron concentrations were below the detection limit on day 0, 0.17 mg L^{-1} on day 22, and 0.10 mg L^{-1} on day 42. Dissolved iron concentrations were under the detection limit for synthetic seawater on day 0 and day 22 (synthetic seawater data could not be collected on day 42). Iron beads will thus not likely leach concerning quantities of iron crosslinkers in environmentally relevant high ionic strength stormwater runoff (*i.e.,* dissolved iron concentrations were even lower than dissolved calcium concentrations in both synthetic stormwater and synthetic seawater). The dissolved iron values measured, however, did not likely constitute all the iron leached from the beads. Specifically, visible brown iron precipitates were present in the synthetic seawater, whereas no precipitates were visible in DI water [Fig. S10†]. Ferric beads in DI water yielded a solution pH of ~3.5, whereas the pH was ~6.15 in synthetic seawater (stored in sealed containers; no change in solution pH over the course of 5 months). Iron solubility is strongly associated with the pH and the redox potential of the solution.[67] As the solution container was sealed and there was *de minimis* headspace, the redox potential of the synthetic seawater is unlikely to change due to oxidation due to air presence in the vial (redox potential of seawater[68] varies between 0.7 and 0.8 V). When pH is below 5, dissolved iron can exist as Fe^{3+}, $FeOH^{++}$, and $Fe(OH)^{2+}$, whereas stable dark brown colloidal suspensions of ferric hydroxides precipitate in the pH range of 5 to 8 at equilibrium.[67] Because Ca^{2+} alginate beads and Fe^{3+} alginate beads do not disintegrate even under high ionic strength solution conditions, both the beads could be applied in environmentally relevant field bioretention cells to treat stormwater runoff.

The durability of the beads in the field environment may not be limited by ion exchange but by microbial degradation.

Because alginate is a natural organic polymer, the alginate in the beads may eventually be degraded in GSI by soil microbes. Very slow biodegradation of dried alginate beads (with no materials encapsulated, made with 2% sodium alginate and 1% $CaCl_2$) has been reported in a microbe-enriched soil environment.[69] In contrast, in an extremely microbially active environment such as a wastewater treatment bioreactor, alginate beads may only last ~15–30 days.[70] Thus, the encapsulated materials in BioSorp beads may be released in a field setting after an extended period. Nevertheless, we do not consider the likely slow biodegradation of alginate and potential the release of the encapsulated materials as a fatal design flaw for stormwater bioretention applications. From a stormwater management perspective, we wanted to create a non-toxic carrier that could deploy sorptive materials and TOrC biodegrading microorganisms in GSI systems. We envision our beads working as biological seeds and spreading microbes throughout the bioretention cells. Hence, an encapsulation process that fully immobilizes the white rot fungi (does not let fungi spread out in the system) would indeed be counter-productive for stormwater treatment. Additionally, BioSorp beads are strong enough to remain stable to enable bioretention cell bioaugmentation and likely (based on our ionic strength experiments) to achieve the design goal of coupled TOrC sorption with subsequent biodegradation. Additional testing under environmentally relevant field conditions will evaluate durability of deployed beads.

3.3 Bioaugmentation potentials of BioSorp beads.

3.3.1 Viability of encapsulated fungi. White rot fungi (WRF) were able to remain viable in the BioSorp beads and could grow from the beads following an extended dried storage period, which is critical for practical bioaugmentation efforts. We successfully encapsulated *Trametes versicolor* fungi in our beads along with PAC, FeWTR, wood flour, and AQDS by entrapping fungi in either Ca^{2+} alginate or Fe^{3+} alginate crosslinkers. When added to growth media (malt extract media and modified Kirk's liquid culture media[71] in this case), dried BioSorp beads were capable of growing fungal fruiting bodies on the surface of the beads [Fig. 6], thereby demonstrating viability of the encapsulated organisms (*i.e.*, no microbial growth occurred in beads that did not contain any fungal culture). We also observed that WRF diffused out of the dried BioSorp beads into the culture media through the cracks and pores, demonstrating potential for bio-augmenting the bioretention cells. Encapsulation is known to increase the shelf life of microorganisms.[72] We maintained our air-dried beads in sealed tubes at room temperature for three months and observed similar fungal growth from stored beads and freshly prepared beads. This extended storage scenario has also been observed for alginate coated entomopathogenic fungus (*Metarhizium anisopliae*), where the authors reported fungal growth even after ten months.[73] Fungal viability can reportedly be substantially increased by storing beads refrigerated (at ~4–5 deg C).[47]

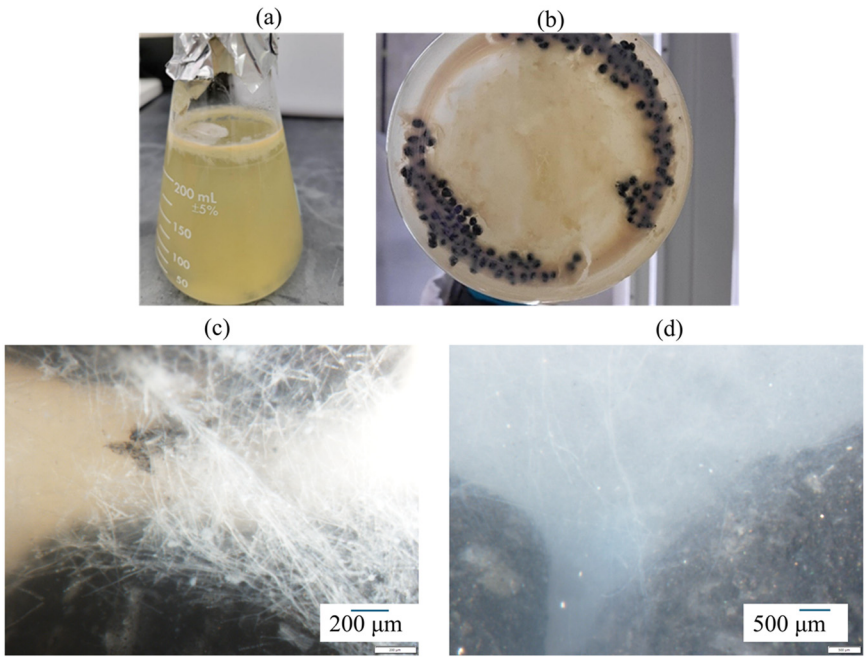

Fig. 6 White rot fungi can grow from the BioSorp beads, demonstrating viability following drying and extended storage periods (*i.e.*, 3 months). (a) and (b) *Trametes versicolor* grew from the BioSorp beads (made with 1% sodium alginate, 1% powder activated carbon, 1% wood flour, and 3% $CaCl_2$) when the beads were kept in malt extract media, (c) closeup stereoscope image of *T. versicolor* growth from BioSorp beads (made with 1% sodium alginate, 1% powder activated carbon, 1% wood flour, and 3% $CaCl_2$), (d) closeup stereoscope image of *T. versicolor* growth from BioSorp beads (made with 1% sodium alginate, 1% powder activated carbon, 1% wood flour, 1% iron water treatment residual, and 3% $CaCl_2$).

The viability of encapsulated fungi appears robust. We prepared oven-dried beads to investigate if bead drying could be accelerated; air drying took ~2–3 days, whereas oven drying took ~8 hours. Because heat is a common environmental stressor, we decided to check fungal viability in the oven dried beads. We observed similar fungal growth for both air-dried and oven-dried beads (OD_{600} was 1.5 after two weeks of bead inoculation into malt extract media). Encapsulation is known to protect microorganisms by providing a higher resistance to the environment.[74] This was evident in the case of our oven-dried beads. Even though the oven-dried beads were dried at 70 degrees Celsius for 8 hours, we did not observe any visible decline in fungal growth compared to the air-dried beads. Freeze drying could also be an alternate process to dry the beads faster but, like oven drying, would require an external energy supply. Encapsulated microorganisms are known to exhibit a decreased tendency to wash out and have higher viability, stability, and activity.[75] Encapsulated microorganisms also reportedly produce more extracellular enzymes that can degrade contaminants outside of the cells.[75] Multiple organic and inorganic polymer matrices could potentially be applied to accomplish this encapsulation process; however, all matrices do not have the same beneficial impacts on microorganisms. Inorganic polymer matrices, such as sol-gels, hold a higher resistance toward microbial and chemical attack and are more durable, but natural organic polymers are non-toxic, biodegradable, and affordable.[76,77] Chitosan is another natural organic polysaccharide (like alginate) that could alternatively be used to encapsulate microorganisms for water treatment.[78] Chitosan powder is often mixed with alginate to increase the mechanical strength of the hybrid gel beads.[79–81]

3.3.2 Creating a beneficial micro-environment to enhance viability and biodegradation. We incorporated wood flour into the BioSorp beads with the goal of providing a maintenance substrate (nutrient supplement) for the fungi to promote longevity when deployed in the field. Loomis *et al.*[47] reported that *Phanerochaete chrysosporium* encapsulated alginate beads (stored at room temperature) exhibited high viability even after nine months when an external nutrient supplement (*i.e.*, wood flour or corncob grits) was present in the bead structure, whereas drastic depletion in viability occurred after only two months in beads that did not contain any nutrient supplementation. This type of maintenance substrate application is not exclusive to WRF and wood flour. For example, shredded straw,[82] grass,[82] newspaper,[83] cotton,[83] rice husk,[84] wood flour,[85] and chlorella[86] have previously been used as external/supplemental carbon sources to increase denitrification in synthetic wastewater and domestic sewage. Maintenance substrates are also reported to increase pollutant removal efficiencies in stormwater bioretention systems. For example, woodchips act as carbon sources and electron donors in biological denitrifying woodchip bioreactors.[87–90] Newspaper (as carbon source and electron donor) has also been added in bioretention cells to improve the stormwater denitrification performance.[91,92] BioSorp beads could also be adaptively prepared by encapsulating alternative carbon sources and contaminant degrading microbes and used for stormwater and/or wastewater treatment applications.

The acidic environment created by ferric alginate beads may specifically promote fungal growth in bioretention cells. Indeed, Johannes *et al.*[93] demonstrated that bacterial and fungal growth in soil were dramatically impacted by variations of pH, where fungal growth increased with decreasing pH (optimum at ~pH 4–5) and bacterial growth increased with increasing pH (optimum at ~pH 7–8). Because Fe^{3+} alginate beads generate lower pH conditions (~3.5) than Ca^{2+} alginate beads (~6.2), Fe^{3+} alginate beads could improve fungal deployment in bioretention cells by creating favorable conditions wherein fungi can more successfully outcompete bacterial biofilms. Fe^{3+} alginate beads could also be suitable for bioaugmenting acidophilic heterotrophic bacteria capable of degrading various aromatic hydrocarbons.[94] Fe^{3+} alginate beads could also potentially facilitate PFAS sorption and biodegradation in bioretention systems (in the presence of adequate NH_4^+ ions) by providing the acidic environment (optimal around pH 4) and Fe^{3+} ions needed by the PFAS-degrading acidophilic Feammox bacteria (*i.e.*, *Acidimicrobium sp.* strain A6).[95] Conversely, calcium alginate beads may be more suitable for bioaugmenting neutrophilic microbes (most bacteria are neutrophiles[96]).

We incorporated AQDS [as external electron shuttles (EES)] in the beads with the goal of enhancing fungal viability potential and biodegradation rates in GSI system. Electron shuttles are capable of reversible oxidation and reduction reactions and can aid biological transformations by acting as redox mediators.[97] Electron shuttles are known to also enhance degradation of some recalcitrant organic contaminants by either donating/accepting electrons for microbial metabolism or donating/accepting electrons to microorganisms for contaminant transformation.[98] Previous studies have reported increased biodegradation of a variety of contaminants in the presence of AQDS. For example, Aulenta *et al.*[99] used AQDS as EES to facilitate microbial dechlorination of trichloroethene (TCE)[102] and Zhou *et al.*[100] demonstrated that AQDS, encapsulated in chitosan gel beads, can provide efficient and environmentally friendly anaerobic decolorization of azo dyes.[103] Thus, the addition of AQDS in BioSorp beads may enhance trace organic biodegradation in bioretention cells. Furthermore, AQDS may also facilitate denitrification in GSI in the presence of ferric sludge (FeWTR). Denitrifying and iron reducing bacteria, present in saturated anaerobic bioretention zone, can use AQDS and iron oxide rich FeWTR to stimulate dissolved N removal.[43,55,101–103] PAC itself can also act as an electron shuttle by accepting and/or donating electrons because of the condensed conjugated pi-electrons present in the structure.[98,104] We will conduct further testing to quantify the impacts of AQDS on contaminant biodegradation in our future studies. Fungal viability in bioretention cell may further improve because PAC can act as growth surface for the biofilms.[105]

3.4 BioSorp beads as a platform technology

We view the work presented herein as a first proof-of-concept for enabling targeted microorganism deployments, *i.e.*, bioaugmentation specifically designed for GSI applications; however, the BioSorp beads are fundamentally platform technology. BioSorp beads are able to provide favorable micro-environments for microbial growth and bioaugmentation. The beads are made of non-toxic materials (*i.e.*, alginate), are physically durable, and incorporate valorized/recycled waste products[84] (*i.e.*, ferric sludge, wood flour). Because the production process is economical and scalable, the bead—through tuning of materials and encapsulated organisms—can be practically applied and adapted for field bioaugmentation.

The sorptive materials used in the beads could also be potentially interchanged with other types of sorptive materials, such as powdered biochar,[18] aluminum-based water treatment residuals,[106] iron oxide coated sorbents,[107] zinc oxide coated sorbents,[108] manganese oxide coated sand,[109,110] *etc.* to specifically tune capture different contaminants. Because our design goal for the beads was stormwater treatment, we decided to use iron-based sorptive materials because iron materials have previously been applied for dissolved P removal in stormwater[111,112] and because Al- or Zn-based sorbents hold the risks of spreading toxic Al or Zn metals[113,114] in the environment. Because coagulant dosage can change according to needs and the influent water quality, the characteristics of FeWTR may also vary temporally or if sourced from different water treatment plants; however, FeWTR would still be produced from iron-based water treatment processes.[43] Powdered iron oxides could alternatively be used in the beads instead of FeWTR to potentially control performance more carefully.[44–46] Because incorporating FeWTR enables valorization of a common waste product and lowers costs in scaled production, we decided to use FeWTR in our beads.

Although we specifically encapsulated white rot fungi in this study as the model bioaugmentation organism for the design application goal in green stormwater infrastructure, the BioSorp bead could easily be modified to encapsulate other types of fungal or bacterial species for specific needs. For example, BioSorp beads containing denitrifying bacteria could be incorporated in the bottom anaerobic saturated zones found in some bioretention designs,[115–117] while beads containing nitrifying bacteria could be added to the upper aerobic unsaturated bioretention zones to maximize nitrogen nutrient removal from stormwater runoff. Along with AQDS, the encapsulated black carbon (PAC) itself or other black carbons could also facilitate redox mediation.[37] Because AQDS is a model electron shuttle and can enhance biodegradation of many recalcitrant TOrCs,[48] we elected to also deploy AQDS to additionally support biodegradation reactions.

BioSorp beads are a platform technology potentially able to encapsulate and deploy multiple types of microorganisms or nutrients for a variety of wastewater or other biotechnology applications. The bead physical properties could also be tuned according to specific needs by adjusting alginate and/or crosslinker concentrations and crosslinker types. One example potential application of BioSorp beads could be incorporation into fluidized bed reactors (FBR), a highly effective technology to treat high strength wastewater.[118,119] Some key challenges while operating FBR are preventing microbial washout, retaining active biomass, and maintaining minimum substrate concentrations needed to sustain microbial redox reactions. BioSorp beads could address this problem by working as microbial seeds and/or reservoirs by retaining the encapsulated microorganisms in FBR system. Preventing microbial washout is also critically important for slow growing microorganisms, such as anammox bacteria (capable of removing high strength ammonia from wastewater).[84] Another possible application of adapted BioSorp beads could be in bioremediation of hazardous materials.[120] Along with contaminant degrading microorganisms, critical limiting micronutrients/vitamins for biodegradation of many hazardous materials could also be incorporated into the beads. For example, encapsulated vitamin B_{12} and PCB degrading microorganisms could potentially enhance and sustain both chemical and microbial reductive dechlorination of PCBs in contaminated sediments.[121]

3.5 Preliminary performance results: efficacy of BioSorp bead sorption

Because encapsulation of sorptive materials can decrease surface area, as we observed herein, we conducted a preliminary investigation of the BioSorp beads sorption efficacy. We selected imidacloprid as a representative hydrophilic TOrC and conducted sorption experiments with several types of abiotic beads (*i.e.,* did not contain any fungi) to quantify BioSorp bead's contaminant capture capability. Imidacloprid is a neonicotinoid insecticide (representative highly polar TOrC; $\log K_{ow}$ = 0.57) that is frequently applied in urban gardens, lawns, and for treating household pets and thus commonly detected in urban stormwater.[122] Here, we spiked imidacloprid in synthetic stormwater to create a solution of contaminated runoff (imidacloprid concentration = ~30 mg L^{-1}). We transferred 100 mL of the prepared contaminated stormwater in serum vials and added 100 mg of BioSorp Beads to each vial. After sealing the vial tops, we maintained the vials on a platform shaker in the dark for ~two weeks (until equilibrium is reached, based on prior work[122]). We used the modified Langmuir equation[122] to predict the maximum sorption capacities for two representative BioSorp beads in this proof-of concept preliminary experiment.

Encapsulation of the sorptive materials did decrease sorption capacity, but much less than the decreased surface area would predict. Imidacloprid sorption capacity for the PAC_WF_WTR_$CaCl_2$ bead was 25.52 mg g^{-1} (bead recipe: 1% alginate, 1% PAC, 1% WF, 1% FeWTR, and 270.3 mM

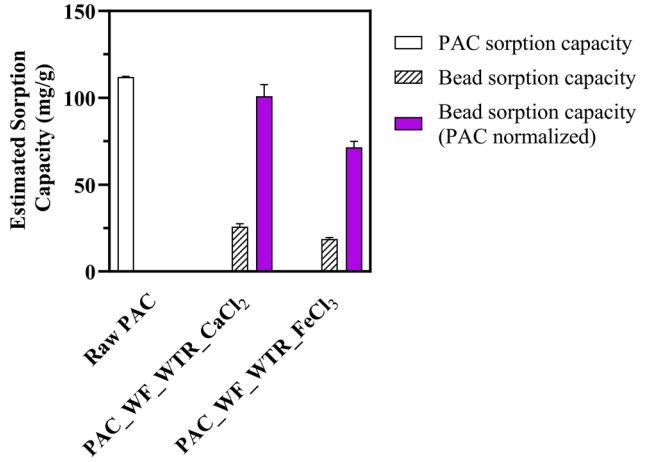

Fig. 7 Imidacloprid sorption capacities of raw PAC and BioSorp beads (n = 3 experimental replicates; error bars represent standard errors of the means. Some error bars are obscured by the data bar plots as the error bars are small). Here, PAC = powdered activated carbon, WF = wood flour, WTR = iron water treatment residuals.

$CaCl_2$) and 18.52 mg g^{-1} for the PAC_WF_WTR_$FeCl_3$ bead (bead recipe: 1% alginate, 1% PAC, 1% WF, 1% FeWTR, and 270.3 mM $FeCl_3$). We determined the imidacloprid sorption capacity for this raw PAC (112 mg g^{-1}) in one of our previous studies.[122] When we normalized the sorption capacities with respect to the mass of PAC in the beads, sorption capacities of PAC_WF_WTR_$CaCl_2$ beads and PAC_WF_WTR_$FeCl_3$ beads were 99.53 mg g^{-1} and 70.93 mg g^{-1}, respectively. Thus, even though the average surface area loss in the beads was ~87% (with respect to raw PAC), average PAC normalized imidacloprid sorption capacity loss was only ~23% [Fig. 7]. It is likely that some of PAC's sorption sites were blocked during encapsulation, thereby limiting imidacloprid sorption. The lower imidacloprid sorption onto PAC_WF_WTR_$FeCl_3$ beads compared to PAC_WF_WTR_$CaCl_2$ beads may relate to the denser crosslinked hydrogel formation in Fe beads than in Ca beads. In our future work, we will quantify detailed sorption values for a suite of TOrCs and dissolved nutrients relevant to urban stormwater and probe coupled sorption and biodegradation *via* the BioSorp beads.

4. Conclusions

The main objective of this research was to develop a cost-effective method to enable rapid capture and subsequent sustained biodegradation of dissolved contaminants while delivering contaminant-degrading microorganisms (*i.e.*, bioaugmentation) in green stormwater infrastructure. We developed a novel composite alginate bead media (*i.e.,* 'BioSorp bead') containing PAC, WRF, wood flour, AQDS, and iron-based water treatment residuals, and demonstrated the bead's potential toward the application design goal of bioaugmenting GSI. This mechanically robust novel assemblage of materials holds promise to enable bioaugmentation and sustained contaminant degradation in GSI, including bioretention cells, without compromising hydraulic conductivity needed for rapid infiltration. Bead properties, such as surface area, pore volume, mechanical strength, *etc.* are customizable and vary with respect to the changes in the recipes. We also demonstrated that white rot fungi remain viable in a protected microenvironment created by the encapsulated conditions and thus BioSorp beads have the practical potential to bioaugment GSI and provide superior stormwater treatment than traditional management systems.

Urban stormwater is well-known to contain a diverse suite of contaminants that have deleterious impacts on the environment.[1] The short hydraulic residence time and low sorption potential associated with most high-hydraulic conductivity, sand-based porous media in GSI perform poorly at removing many dissolved phase contaminants, including polar trace organics and dissolved nutrients, thereby generating concomitant risk for groundwater contamination.[3] Indeed, amended bioretention media are capable of capturing increased quantities of trace organic contaminants.[123] BioSorp beads could be incorporated into new bioretention systems or amended post-construction into existing GSI systems for bioaugmentation. BioSorp beads are designed to directly address the wicked problem of hydrophilic compounds by: (1) rapidly capturing contaminants onto the black carbon materials *via* chemical sorption during the rapid infiltration stages and (2) encapsulating and bioaugmenting contaminant degrading microorganisms in GSI systems. Even if some of the non-toxic encapsulated materials or microorganisms (presuming selection of non-invasive species) were to eventually leach from the beads in the field, coupled contaminant sorption and biodegradation are likely to occur simultaneously in bioretention cells and be benefited by the presence of materials. For example, a recent study estimated that black carbon amended biofilters (5% biochar, v/v) could sustain TOrC removal for at least 17 years before the effluent water quality dropped to the levels that pose threats to aquatic lives.[24] Further field-scale studies will be required to accurately quantify lifetimes of BioSorp beads in field bioretention cells. We posit that synergizing rapid chemical capture during storm events with subsequent, slower biodegradation during inter-storm periods could optimize GSI system performance by maximizing stormwater volume infiltrated and contaminant mass removed. Decoupling the hydraulic residence time from contaminant residence time using BioSorp beads could elevate GSI performance for hydrophilic organic contaminants, in much the same way activated sludge revolutionized wastewater treatment by decoupling hydraulic residence time from solids retention time. Our future research will quantify the performance of these beads for contaminant sorption and biodegradation.

Author contributions

Debojit S. Tanmoy: conceptualization, methodology, software, formal analysis, investigation, data curation, writing – original draft, visualization, project administration. Gregory H. LeFevre: conceptualization, methodology, resources, writing – review & editing, supervision, project administration, funding acquisition.

Conflicts of interest

There are no conflicts of interest to declare.

Acknowledgements

This work was supported by the National Science Foundation CBET CAREER under Grant 1844720. The authors would like to thank Dr. Drew E. Latta (University of Iowa), Dr. Alexei V. Tivanski (University of Iowa), the UI CMRF, and the UI MATFab Facility.

References

1 L. Mutzner, K. Zhang, R. G. Luthy, H. P. H. Arp and S. Spahr, Urban stormwater capture for water supply: look out for persistent, mobile and toxic substances, *Environ. Sci.: Water Res. Technol.*, 2023, **9**, 3094–3102.

2 Z. Kong, Y. Song, Z. Shao and H. Chai, Biochar-pyrite bi-layer bioretention system for dissolved nutrient treatment and by-product generation control under various stormwater conditions, *Water Res.*, 2021, **206**, 117737.

3 T. F. M. Rodgers, L. Wu, X. Gu, S. Spraakman, E. Passeport and M. L. Diamond, Stormwater Bioretention Cells Are Not an Effective Treatment for Persistent and Mobile Organic Compounds (PMOCs), *Environ. Sci. Technol.*, 2022, **56**, 6349–6359.

4 M. E. Dietz, Low Impact Development Practices: A Review of Current Research and Recommendations for Future Directions, *Water, Air, Soil Pollut.*, 2007, **186**, 351–363.

5 S. Alam, A. Borthakur, S. Ravi, M. Gebremichael and S. K. Mohanty, Managed aquifer recharge implementation criteria to achieve water sustainability, *Sci. Total Environ.*, 2021, **768**, 144992.

6 P. Jokela and E. Kallio, Sprinkling and Well Infiltration in Managed Aquifer Recharge for Drinking Water Quality Improvement in Finland, *J. Hydrol. Eng.*, 2015, **20**(3), DOI: **10.1061/(ASCE)HE.1943-5584.0000975**.

7 C. Yoo, J. M. Ku, C. Jun and J. H. Zhu, Simulation of infiltration facilities using the SEEP/W model and quantification of flood runoff reduction effect by the decrease in CN, *Water Sci. Technol.*, 2016, **74**, 118–129.

8 G. H. LeFevre, M. D. Hendricks, M. E. Carrasquillo, L. E. McPhillips, B. K. Winfrey and J. R. Mihelcic, The Greatest Opportunity for Green Stormwater Infrastructure Is to Advance Environmental Justice, *Environ. Sci. Technol.*, 2023, **57**, 19088–19093.

9 A. Dietrich, R. Yarlagadda and C. Gruden, Estimating the potential benefits of green stormwater infrastructure on developed sites using hydrologic model simulation, *Environ. Prog. Sustainable Energy*, 2017, **36**, 557–564.

10 J. Liu, D. J. Sample, C. Bell and Y. Guan, Review and Research Needs of Bioretention Used for the Treatment of Urban Stormwater, *Water*, 2014, **6**, 1069–1099.

11 C. M. Rodak, T. L. Moore, R. David, A. D. Jayakaran and J. R. Vogel, Urban stormwater characterization, control, and treatment, *Water Environ. Res.*, 2019, **91**, 1034–1060.

12 C. Hsieh and A. P. Davis, Evaluation and optimization of bioretention media for treatment of urban storm water runoff, *J. Environ. Eng.*, 2005, **131**, 1521–1531.

13 J. R. Masoner, D. W. Kolpin, I. M. Cozzarelli, L. B. Barber, D. S. Burden, W. T. Foreman, K. J. Forshay, E. T. Furlong, J. F. Groves, M. L. Hladik, M. E. Hopton, J. B. Jaeschke, S. H. Keefe, D. P. Krabbenhoft, R. Lowrance, K. M. Romanok, D. L. Rus, W. R. Selbig, B. H. Williams and P. M. Bradley, Urban Stormwater: An Overlooked Pathway of Extensive Mixed Contaminants to Surface and Groundwaters in the United States, *Environ. Sci. Technol.*, 2019, **53**, 10070–10081.

14 S. M. Elliott, R. L. Kiesling, A. M. Berg and H. L. Schoenfuss, A pilot study to assess the influence of infiltrated stormwater on groundwater: Hydrology and trace organic contaminants, *Water Environ. Res.*, 2022, **94**(2), DOI: **10.1002/wer.10690**.

15 A. Behbahani, R. J. Ryan and E. R. McKenzie, Long-term simulation of potentially toxic elements (PTEs) accumulation and breakthrough in infiltration-based stormwater management practices (SMPs), *J. Contam. Hydrol.*, 2020, **234**, 103685.

16 A. Zubair, A. Hussain, M. A. Farooq and H. N. Abbasi, Impact of storm water on groundwater quality below retention/detention basins, *Environ. Monit. Assess.*, 2010, **162**, 427–437.

17 K. Björklund and L. Li, Removal of organic contaminants in bioretention medium amended with activated carbon from sewage sludge, *Environ. Sci. Pollut. Res.*, 2017, **24**, 19167–19180.

18 B. A. Ulrich, E. A. Im, D. Werner and C. P. Higgins, Biochar and Activated Carbon for Enhanced Trace Organic Contaminant Retention in Stormwater Infiltration Systems, *Environ. Sci. Technol.*, 2015, **49**, 6222–6230.

19 M. Hassan, Y. Liu, R. Naidu, S. J. Parikh, J. Du, F. Qi and I. R. Willett, Influences of feedstock sources and pyrolysis temperature on the properties of biochar and functionality as adsorbents: A meta-analysis, *Sci. Total Environ.*, 2020, **744**, 140714.

20 B. A. Ulrich, M. Loehnert and C. P. Higgins, Improved contaminant removal in vegetated stormwater biofilters amended with biochar, *Environ. Sci.: Water Res. Technol.*, 2017, **3**, 726–734.

21 I. LeviRam, A. Gross, A. Lintern, R. Henry, C. Schang, M. Herzberg and D. McCarthy, Sustainable micropollutant bioremediation via stormwater biofiltration system, *Water Res.*, 2022, **214**, 118188.

22 Z. Kong, Y. Song, M. Xu, Y. Yang, X. Wang, H. Ma, Y. Zhi, Z. Shao, L. Chen, Y. Yuan, F. Liu, Y. Xu, Q. Ni, S. Hu and H. Chai, Multi-media interaction improves the efficiency and stability of the bioretention system for stormwater runoff treatment, *Water Res.*, 2024, **250**, 121017.

23 V. K. Vaithyanathan, O. Savary and H. Cabana, Performance evaluation of biocatalytic and biostimulation approaches for the remediation of trace organic contaminants in municipal biosolids, *Waste Manage.*, 2021, **120**, 373–381.

24 A. C. Portmann, G. H. LeFevre, R. Hankawa, D. Werner and C. P. Higgins, The regenerative role of biofilm in the removal of pesticides from stormwater in biochar-amended biofilters, *Environ. Sci.: Water Res. Technol.*, 2022, **8**, 1092–1110.

25 X. Min, W. Li, Z. Wei, R. Spinney, D. D. Dionysiou, Y. Seo, C.-J. Tang, Q. Li and R. Xiao, Sorption and biodegradation of pharmaceuticals in aerobic activated sludge system: A combined experimental and theoretical mechanistic study, *Chem. Eng. J.*, 2018, **342**, 211–219.

26 C. P. Muerdter, C. K. Wong and G. H. LeFevre, Emerging investigator series: the role of vegetation in bioretention for stormwater treatment in the built environment: pollutant removal, hydrologic function, and ancillary benefits, *Environ. Sci.: Water Res. Technol.*, 2018, **4**, 592–612.

27 G. H. LeFevre, R. M. Hozalski and P. J. Novak, The role of biodegradation in limiting the accumulation of petroleum hydrocarbons in raingarden soils, *Water Res.*, 2012, **46**, 6753–6762.

28 G. H. LeFevre, P. J. Novak and R. M. Hozalski, Fate of Naphthalene in Laboratory-Scale Bioretention Cells: Implications for Sustainable Stormwater Management, *Environ. Sci. Technol.*, 2012, **46**, 995–1002.

29 M. B. Asif, F. I. Hai, L. Singh, W. E. Price and L. D. Nghiem, Degradation of Pharmaceuticals and Personal Care Products by White-Rot Fungi—a Critical Review, *Curr. Pollut. Rep.*, 2017, **3**, 88–103.

30 S. Wang, W. Li, L. Liu, H. Qi and H. You, Biodegradation of decabromodiphenyl ethane (DBDPE) by white-rot fungus Pleurotus ostreatus: Characteristics, mechanisms, and toxicological response, *J. Hazard. Mater.*, 2022, **424**, 127716.

31 E. A. Wiener and G. H. LeFevre, White Rot Fungi Produce Novel Tire Wear Compound Metabolites and Reveal Underappreciated Amino Acid Conjugation Pathways, *Environ. Sci. Technol. Lett.*, 2022, **9**, 391–399.

32 C. Rauert, N. Charlton, E. D. Okoffo, R. S. Stanton, A. R. Agua, M. C. Pirrung and K. V. Thomas, Concentrations of Tire Additive Chemicals and Tire Road Wear Particles in an Australian Urban Tributary, *Environ. Sci. Technol.*, 2022, **56**, 2421–2431.

33 M. Brinkmann, D. Montgomery, S. Selinger, J. G. P. Miller, E. Stock, A. J. Alcaraz, J. K. Challis, L. Weber, D. Janz, M. Hecker and S. Wiseman, Acute Toxicity of the Tire Rubber-Derived Chemical 6PPD-quinone to Four Fishes of Commercial, Cultural, and Ecological Importance, *Environ. Sci. Technol. Lett.*, 2022, **9**, 333–338.

34 J. K. McIntyre, J. Prat, J. Cameron, J. Wetzel, E. Mudrock, K. T. Peter, Z. Tian, C. Mackenzie, J. Lundin, J. D. Stark, K. King, J. W. Davis, E. P. Kolodziej and N. L. Scholz, Treading Water: Tire Wear Particle Leachate Recreates an Urban Runoff Mortality Syndrome in Coho but Not Chum Salmon, *Environ. Sci. Technol.*, 2021, **55**, 11767–11774.

35 Z. Tian, H. Zhao, K. T. Peter, M. Gonzalez, J. Wetzel, C. Wu, X. Hu, J. Prat, E. Mudrock, R. Hettinger, A. E. Cortina, R. G. Biswas, F. V. C. Kock, R. Soong, A. Jenne, B. Du, F. Hou, H. He, R. Lundeen, A. Gilbreath, R. Sutton, N. L. Scholz, J. W. Davis, M. C. Dodd, A. Simpson, J. K. McIntyre and E. P. Kolodziej, A ubiquitous tire rubber–derived chemical induces acute mortality in coho salmon, *Science*, 2021, **371**, 185–189.

36 J. M. Wolfand, G. H. LeFevre and R. G. Luthy, Metabolization and degradation kinetics of the urban-use pesticide fipronil by white rot fungus Trametes versicolor, *Environ. Sci.: Processes Impacts*, 2016, **18**, 1256–1265.

37 S. Mukherjee, B. Sarkar, V. K. Aralappanavar, R. Mukhopadhyay, B. B. Basak, P. Srivastava, O. Marchut-Mikołajczyk, A. Bhatnagar, K. T. Semple and N. Bolan, Biochar-microorganism interactions for organic pollutant remediation: Challenges and perspectives, *Environ. Pollut.*, 2022, **308**, 119609.

38 D. Pandey, A. Daverey and K. Arunachalam, Biochar: Production, properties and emerging role as a support for enzyme immobilization, *J. Cleaner Prod.*, 2020, **255**, 120267.

39 E. Taskin, M. T. Branà, C. Altomare and E. Loffredo, Biochar and hydrochar from waste biomass promote the growth and enzyme activity of soil-resident ligninolytic fungi, *Heliyon*, 2019, **5**, e02051.

40 C. J. Mitchell, A. D. Jayakaran and J. K. McIntyre, Biochar and fungi as bioretention amendments for bacteria and PAH removal from stormwater, *J. Environ. Manage.*, 2023, **327**, 116915.

41 A. Taylor, J. Wetzel, E. Mudrock, K. King, J. Cameron, J. Davis and J. McIntyre, Engineering Analysis of Plant and Fungal Contributions to Bioretention Performance, *Water*, 2018, **10**, 1226.

42 D. Mohapatra, S. K. Rath and P. K. Mohapatra, in *Mycoremediation and Environmental Sustainability*, ed. R. Prasad, Springer International Publishing, Cham, 2018, vol. 2, pp. 181–212.

43 R. Sanchis, A. Dejoz, I. Vázquez, E. Vilarrasa-García, J. Jiménez-Jiménez, E. Rodríguez-Castellón, J. M. López Nieto and B. Solsona, Ferric sludge derived from the process of water purification as an efficient catalyst and/or support for the removal of volatile organic compounds, *Chemosphere*, 2019, **219**, 286–295.

44 H. Smaili and C. Ng, Adsorption as a remediation technology for short-chain per- and polyfluoroalkyl substances (PFAS) from water – a critical review, *Environ. Sci.*, 2023, **9**, 344–362.

45 H. Lin, Y. Wang, J. Niu, Z. Yue and Q. Huang, Efficient Sorption and Removal of Perfluoroalkyl Acids (PFAAs) from Aqueous Solution by Metal Hydroxides Generated in Situ by Electrocoagulation, *Environ. Sci. Technol.*, 2015, **49**, 10562–10569.

46 M. K. Gibbons and G. A. Gagnon, Understanding removal of phosphate or arsenate onto water treatment residual solids, *J. Hazard. Mater.*, 2011, **186**, 1916–1923.

47 A. K. Loomis, A. M. Childress, D. Daigle and J. W. Bennett, Alginate Encapsulation of the White Rot Fungus Phanerochaete chrysosporium, *Curr. Microbiol.*, 1997, **34**, 127–130.

48 Z. Chen, Y. Wang, X. Jiang, D. Fu, D. Xia, H. Wang, G. Dong and Q. Li, Dual roles of AQDS as electron shuttles for

microbes and dissolved organic matter involved in arsenic and iron mobilization in the arsenic-rich sediment, *Sci. Total Environ.*, 2017, **574**, 1684–1694.

49 L. E. de-Bashan and Y. Bashan, Immobilized microalgae for removing pollutants: Review of practical aspects, *Bioresour. Technol.*, 2010, **101**, 1611–1627.

50 V. Rocher, J.-M. Siaugue, V. Cabuil and A. Bee, Removal of organic dyes by magnetic alginate beads, *Water Res.*, 2008, **42**, 1290–1298.

51 B. Wang, Y. Wan, Y. Zheng, X. Lee, T. Liu, Z. Yu, J. Huang, Y. S. Ok, J. Chen and B. Gao, Alginate-based composites for environmental applications: a critical review, *Crit. Rev. Environ. Sci. Technol.*, 2019, **49**, 318–356.

52 D. Massana Roquero, A. Othman, A. Melman and E. Katz, Iron(iii)-cross-linked alginate hydrogels: a critical review, *Mater. Adv.*, 2022, **3**, 1849–1873.

53 P. Nandanwar, R. Jugade, V. Gomase, A. Shekhawat, A. Bambal, D. Saravanan and S. Pandey, Chitosan-Biopolymer-Entrapped Activated Charcoal for Adsorption of Reactive Orange Dye from Aqueous Phase and CO2 from Gaseous Phase, *J. Compos. Sci.*, 2023, **7**, 103.

54 S. Peretz, D. F. Anghel, E. Vasilescu, M. Florea-Spiroiu, C. Stoian and G. Zgherea, Synthesis, characterization and adsorption properties of alginate porous beads, *Polym. Bull.*, 2015, **72**, 3169–3182.

55 F. J. Cervantes, C. H. Gutiérrez, K. Y. López, M. I. Estrada-Alvarado, E. R. Meza-Escalante, A.-C. Texier, F. Cuervo and J. Gómez, Contribution of quinone-reducing microorganisms to the anaerobic biodegradation of organic compounds under different redox conditions, *Biodegradation*, 2008, **19**, 235–246.

56 J. A. Field, Recalcitrance as a catalyst for new developments, *Water Sci. Technol.*, 2001, **44**, 33–40.

57 A. B. dos Santos, F. J. Cervantes and J. B. van Lier, Azo dye reduction by thermophilic anaerobic granular sludge, and the impact of the redox mediator anthraquinone-2,6-disulfonate (AQDS) on the reductive biochemical transformation, *Appl. Microbiol. Biotechnol.*, 2004, **64**, 62–69.

58 K. He, Q. Yin, A. Liu, S. Echigo, S. Itoh and G. Wu, Enhanced anaerobic degradation of amide pharmaceuticals by dosing ferroferric oxide or anthraquinone-2, 6-disulfonate, *J. Water Process Eng.*, 2017, **18**, 192–197.

59 A. Kumar and H. M. Jena, Preparation and characterization of high surface area activated carbon from Fox nut (Euryale ferox) shell by chemical activation with H3PO4, *Results Phys.*, 2016, **6**, 651–658.

60 M. Thommes, K. Kaneko, A. V. Neimark, J. P. Olivier, F. Rodriguez-Reinoso, J. Rouquerol and K. S. W. Sing, *Physisorption of gases, with special reference to the evaluation of surface area and pore size distribution (IUPAC Technical Report)*, 2015, vol. 87, pp. 1051–1069.

61 E.-S. Chan, T.-K. Lim, W.-P. Voo, R. Pogaku, B. T. Tey and Z. Zhang, Effect of formulation of alginate beads on their mechanical behavior and stiffness, *Particuology*, 2011, **9**, 228–234.

62 W.-P. Voo, C.-W. Ooi, A. Islam, B.-T. Tey and E.-S. Chan, Calcium alginate hydrogel beads with high stiffness and extended dissolution behaviour, *Eur. Polym. J.*, 2016, **75**, 343–353.

63 P. Rayment and M. F. Butler, Investigation of ionically crosslinked chitosan and chitosan–bovine serum albumin beads for novel gastrointestinal functionality, *J. Appl. Polym. Sci.*, 2008, **108**, 2876–2885.

64 P. Del Gaudio, P. Colombo, G. Colombo, P. Russo and F. Sonvico, Mechanisms of formation and disintegration of alginate beads obtained by prilling, *Int. J. Pharm.*, 2005, **302**, 1–9.

65 A. Nasrullah, A. H. Bhat, A. Naeem, M. H. Isa and M. Danish, High surface area mesoporous activated carbon-alginate beads for efficient removal of methylene blue, *Int. J. Biol. Macromol.*, 2018, **107**, 1792–1799.

66 S. K. Bajpai and S. Sharma, Investigation of swelling/degradation behaviour of alginate beads crosslinked with Ca2+ and Ba2+ ions, *React. Funct. Polym.*, 2004, **59**, 129–140.

67 J. D. Hem and W. H. Cropper, *Survey of ferrous-ferric chemical equilibria and redox potentials*, US Geological Survey Report Water Supply Paper 1459-A, 1959, DOI: **10.3133/wsp1459A**.

68 L. H. N. Cooper, Oxidation-Reduction Potential in Sea Water, *J. Mar. Biol. Assoc. U. K.*, 1937, **22**, 167–176.

69 Y. Achmon, F. R. Dowdy, C. W. Simmons, C. Zohar-Perez, Z. Rabinovitz and A. Nussinovitch, Degradation and bioavailability of dried alginate hydrocolloid capsules in simulated soil system, *J. Appl. Polym. Sci.*, 2019, **136**, 48142.

70 O. Murujew, R. Whitton, M. Kube, L. Fan, F. Roddick, B. Jefferson and M. Pidou, Recovery and reuse of alginate in an immobilized algae reactor, *Environ. Technol.*, 2021, **42**, 1521–1530.

71 S. Zhu, A. Chen, Y. Chai, R. Cao, J. Zeng, M. Bai, L. Peng, J. Shao and X. Wang, Extracellular enzyme mediated biotransformation of imidacloprid by white-rot fungus Phanerochaete chrysosporium: Mechanisms, pathways, and toxicity, *Chem. Eng. J.*, 2023, **472**, 144798.

72 Q. Sun, S. Yin, Y. He, Y. Cao and C. Jiang, Biomaterials and Encapsulation Techniques for Probiotics: Current Status and Future Prospects in Biomedical Applications, *Nanomaterials*, 2023, **13**, 2185.

73 B. D. Sarma, K. C. Puzari, P. Dutta and A. K. Pandey, An alginate-based encapsulation enhances shelf life and bioactivity of the entomopathogenic fungus, Metarhizium anisopliae, *Egypt. J. Biol. Pest Control*, 2023, **33**, 69.

74 I. Holzmeister, M. Schamel, J. Groll, U. Gbureck and E. Vorndran, Artificial inorganic biohybrids: The functional combination of microorganisms and cells with inorganic materials, *Acta Biomater.*, 2018, **74**, 17–35.

75 M. V. Tuttolomondo, G. S. Alvarez, M. F. Desimone and L. E. Diaz, Removal of azo dyes from water by sol–gel immobilized Pseudomonas sp, *J. Environ. Chem. Eng.*, 2014, **2**, 131–136.

76 W. Ghach, M. Etienne, P. Billard, F. P. A. Jorand and A. Walcarius, Electrochemically assisted bacteria encapsulation in thin hybrid sol–gel films, *J. Mater. Chem. B*, 2013, **1**, 1052–1059.

77 T. Mehrotra, S. Dev, A. Banerjee, A. Chatterjee, R. Singh and S. Aggarwal, Use of immobilized bacteria for environmental

bioremediation: A review, *J. Environ. Chem. Eng.*, 2021, **9**, 105920.
78 S. H. Lau, I.-C. Lin, C.-L. Su, Y.-T. Chang and W.-N. Jane, Synthesis of cross-linked magnetic chitosan beads immobilised with bacteria for aerobic biodegrading benzophenone-type UV filter, *Chemosphere*, 2022, **307**, 136010.
79 P. Ngamsurach, N. Namwongsa and P. Praipipat, Synthesis of powdered and beaded chitosan materials modified with ZnO for removing lead (II) ions, *Sci. Rep.*, 2022, **12**, 17184.
80 B. Qu and Y. Luo, Chitosan-based hydrogel beads: Preparations, modifications and applications in food and agriculture sectors – A review, *Int. J. Biol. Macromol.*, 2020, **152**, 437–448.
81 J. Wang and S. Zhuang, Removal of various pollutants from water and wastewater by modified chitosan adsorbents, *Crit. Rev. Environ. Sci. Technol.*, 2017, **47**, 2331–2386.
82 B. Zhou, J. Duan, L. Xue, J. Zhang and L. Yang, Effect of plant-based carbon source supplements on denitrification of synthetic wastewater: focus on the microbiology, *Environ. Sci. Pollut. Res.*, 2019, **26**, 24683–24694.
83 Z. Si, X. Song, Y. Wang, X. Cao, Y. Zhao, B. Wang, Y. Chen and A. Arefe, Intensified heterotrophic denitrification in constructed wetlands using four solid carbon sources: Denitrification efficiency and bacterial community structure, *Bioresour. Technol.*, 2018, **267**, 416–425.
84 D. S. Tanmoy, J. C. Bezares-Cruz and G. H. LeFevre, The use of recycled materials in a biofilter to polish anammox wastewater treatment plant effluent, *Chemosphere*, 2022, **296**, 134058.
85 R. Hu, X. Zheng, T. Zheng, J. Xin, H. Wang and Q. Sun, Effects of carbon availability in a woody carbon source on its nitrate removal behavior in solid-phase denitrification, *J. Environ. Manage.*, 2019, **246**, 832–839.
86 F. Zhong, S. Huang, J. Wu, S. Cheng and Z. Deng, The use of microalgal biomass as a carbon source for nitrate removal in horizontal subsurface flow constructed wetlands, *Ecol. Eng.*, 2019, **127**, 263–267.
87 B. J. Halaburka, G. H. LeFevre and R. G. Luthy, Evaluation of Mechanistic Models for Nitrate Removal in Woodchip Bioreactors, *Environ. Sci. Technol.*, 2017, **51**, 5156–5164.
88 B. J. Halaburka, G. H. LeFevre and R. G. Luthy, Quantifying the temperature dependence of nitrate reduction in woodchip bioreactors: experimental and modeled results with applied case-study, *Environ. Sci.: Water Res. Technol.*, 2019, **5**, 782–797.
89 N. Ashoori, M. Teixido, S. Spahr, G. H. LeFevre, D. L. Sedlak and R. G. Luthy, Evaluation of pilot-scale biochar-amended woodchip bioreactors to remove nitrate, metals, and trace organic contaminants from urban stormwater runoff, *Water Res.*, 2019, **154**, 1–11.
90 M. Teixidó, J. A. Charbonnet, G. H. LeFevre, R. G. Luthy and D. L. Sedlak, Use of pilot-scale geomedia-amended biofiltration system for removal of polar trace organic and inorganic contaminants from stormwater runoff, *Water Res.*, 2022, **226**, 119246.
91 H. Kim, E. A. Seagren and A. P. Davis, Engineered Bioretention for Removal of Nitrate from Stormwater Runoff, *Water Environ. Res.*, 2003, **75**, 355–367.
92 H. W. Goh, N. A. Zakaria, T. L. Lau, K. Y. Foo, C. K. Chang and C. S. Leow, Mesocosm study of enhanced bioretention media in treating nutrient rich stormwater for mixed development area, *Urban Water J.*, 2017, **14**, 134–142.
93 J. Rousk, P. C. Brookes and E. Bååth, Contrasting Soil pH Effects on Fungal and Bacterial Growth Suggest Functional Redundancy in Carbon Mineralization, *Appl. Environ. Microbiol.*, 2009, **75**(6), 1589–1596.
94 R. D. Stapleton, D. C. Savage, G. S. Sayler and G. Stacey, Biodegradation of Aromatic Hydrocarbons in an Extremely Acidic Environment, *Appl. Environ. Microbiol.*, 1998, **64**, 4180–4184.
95 S. Huang and P. R. Jaffé, Defluorination of Perfluorooctanoic Acid (PFOA) and Perfluorooctane Sulfonate (PFOS) by Acidimicrobium sp. Strain A6, *Environ. Sci. Technol.*, 2019, **53**, 11410–11419.
96 W. Keenleyside, *Microbiology: Canadian Edition*, Pressbooks, 2019.
97 K. Watanabe, M. Manefield, M. Lee and A. Kouzuma, Electron shuttles in biotechnology, *Curr. Opin. Biotechnol.*, 2009, **20**, 633–641.
98 L. Zhou, T. Chi, Y. Zhou, H. Chen, C. Du, G. Yu, H. Wu, X. Zhu and G. Wang, Stimulation of pyrolytic carbon materials as electron shuttles on the anaerobic transformation of recalcitrant organic pollutants: A review, *Sci. Total Environ.*, 2021, **801**, 149696.
99 F. Aulenta, V. Di Maio, T. Ferri and M. Majone, The humic acid analogue antraquinone-2,6-disulfonate (AQDS) serves as an electron shuttle in the electricity-driven microbial dechlorination of trichloroethene to cis-dichloroethene, *Bioresour. Technol.*, 2010, **101**, 9728–9733.
100 W. Zhou, X. Chen, M. Ismail, L. Wei and B. Hu, Simulating the synergy of electron donors and different redox mediators on the anaerobic decolorization of azo dyes: Can AQDS-chitosan globules replace the traditional redox mediators?, *Chemosphere*, 2021, **275**, 130025.
101 J. Xia, Y. Li, X. Jiang, D. Chen and J. Shen, The humic substance analogue antraquinone-2, 6-disulfonate (AQDS) enhanced zero-valent iron based autotrophic denitrification: Performances and mechanisms, *Environ. Res.*, 2023, **238**, 117241.
102 G. Wang, Z. Teng, X. Zhao, W. Luo, J. Liang, Y. Guo, X. Ji, W. Hu and M. Li, AQDS-mediated dissimilatory reduction of iron (hydr)oxides induces the formation of large grain vivianite: A new insight for phosphorus pollution control in sediment, *J. Cleaner Prod.*, 2023, **419**, 138217.
103 K. L. Straub, A. Kappler and B. Schink, Enrichment and Isolation of Ferric-Iron- and Humic-Acid-Reducing Bacteria, *Methods Enzymol.*, 2005, **397**, 58–77.
104 L. Klüpfel, M. Keiluweit, M. Kleber and M. Sander, Redox Properties of Plant Biomass-Derived Black Carbon (Biochar), *Environ. Sci. Technol.*, 2014, **48**, 5601–5611.

105 L. G. Bó, R. M. Almeida, C. M. M. Cardoso, D. G. Zavarize, S. S. Brum and A. R. V. Mendonça, Acetylsalicylic acid biosorption onto fungal-bacterial biofilm supported on activated carbons: an investigation via batch and fixed-bed experiments, *Environ. Sci. Pollut. Res.*, 2019, **26**, 28962–28976.

106 J. A. Leiva, P. C. Wilson, J. P. Albano, P. Nkedi-Kizza and G. A. O'Connor, Pesticide Sorption to Soilless Media Components Used for Ornamental Plant Production and Aluminum Water Treatment Residuals, *ACS Omega*, 2019, **4**, 17782–17790.

107 Lalhmunsiama, R. R. Pawar, S.-M. Hong, K. J. Jin and S.-M. Lee, Iron-oxide modified sericite alginate beads: A sustainable adsorbent for the removal of As(V) and Pb(II) from aqueous solutions, *J. Mol. Liq.*, 2017, **240**, 497–503.

108 S. Vahidhabanu, D. Karuppasamy, A. I. Adeogun and B. R. Babu, Impregnation of zinc oxide modified clay over alginate beads: a novel material for the effective removal of congo red from wastewater, *RSC Adv.*, 2017, **7**, 5669–5678.

109 J. E. Grebel, J. A. Charbonnet and D. L. Sedlak, Oxidation of organic contaminants by manganese oxide geomedia for passive urban stormwater treatment systems, *Water Res.*, 2016, **88**, 481–491.

110 J. A. Charbonnet, Y. Duan, C. M. van Genuchten and D. L. Sedlak, Chemical Regeneration of Manganese Oxide-Coated Sand for Oxidation of Organic Stormwater Contaminants, *Environ. Sci. Technol.*, 2018, **52**, 10728–10736.

111 A. J. Erickson, J. S. Gulliver and P. T. Weiss, Capturing phosphates with iron enhanced sand filtration, *Water Res.*, 2012, **46**, 3032–3042.

112 A. Erickson, J. Gulliver and P. Weiss, Phosphate Removal from Agricultural Tile Drainage with Iron Enhanced Sand, *Water*, 2017, **9**, 672.

113 R. H. Alasfar and R. J. Isaifan, Aluminum environmental pollution: the silent killer, *Environ. Sci. Pollut. Res.*, 2021, **28**, 44587–44597.

114 L. A. Kszos, G. W. Morris and B. K. Konetsky, Source of toxicity in storm water: Zinc from commonly used paint, *Environ. Toxicol. Chem.*, 2004, **23**, 12–16.

115 L. J. Waller, G. K. Evanylo, L.-A. H. Krometis, M. S. Strickland, T. Wynn-Thompson and B. D. Badgley, Engineered and Environmental Controls of Microbial Denitrification in Established Bioretention Cells, *Environ. Sci. Technol.*, 2018, **52**, 5358–5366.

116 A. G. Donaghue, N. Morgan, L. Toran and E. R. McKenzie, The impact of bioretention column internal water storage underdrain height on denitrification under continuous and transient flow, *Water Res.*, 2022, **214**, 118205.

117 S. Wang, X. Lin, H. Yu, Z. Wang, H. Xia, J. An and G. Fan, Nitrogen removal from urban stormwater runoff by stepped bioretention systems, *Ecol. Eng.*, 2017, **106**, 340–348.

118 C. Mallikarjuna and R. R. Dash, A review on hydrodynamic parameters and biofilm characteristics of inverse fluidized bed bioreactors for treating industrial wastewater, *J. Environ. Chem. Eng.*, 2020, **8**, 104233.

119 M. Alsubih, R. El Morabet, R. A. Khan, N. A. Khan, A. R. Khan and G. Sharma, Performance evaluation of aerobic fluidized bed bioreactor coupled with tube-settler for hospital wastewater treatment, *J. Environ. Chem. Eng.*, 2021, **9**, 105896.

120 US EPA, *What is Superfund*, https://www.epa.gov/superfund/what-superfund, (accessed 26 February 2024).

121 S. L. Woods, D. J. Trobaugh and K. J. Carter, Polychlorinated Biphenyl Reductive Dechlorination by Vitamin B12s: Thermodynamics and Regiospecificity, *Environ. Sci. Technol.*, 1999, **33**, 857–863.

122 D. T. Webb, M. R. Nagorzanski, M. M. Powers, D. M. Cwiertny, M. L. Hladik and G. H. LeFevre, Differences in Neonicotinoid and Metabolite Sorption to Activated Carbon Are Driven by Alterations to the Insecticidal Pharmacophore, *Environ. Sci. Technol.*, 2020, **54**, 14694–14705.

123 T. F. M. Rodgers, S. Spraakman, Y. Wang, C. Johannessen, R. C. Scholes and A. Giang, Bioretention Design Modifications Increase the Simulated Capture of Hydrophobic and Hydrophilic Trace Organic Compounds, *Environ. Sci. Technol.*, 2024, **58**, 5500–5511.